Transparency and imaginary colors

Whitman Richards,[1,*] Jan J. Koenderink,[2] and Andrea van Doorn[3]

[1]*Massachusetts Institute of Technology, 32-364, Cambridge, Massachusetts 02139, USA*
[2]*Delft University of Technology, Faculty of EEMCS Mekelweg 4, 2628 CD Delft, The Netherlands*
[3]*Delft University of Technology, Faculty of Industrial Design Landbergstraat 15, 2628 CE Delft, The Netherlands*
**Corresponding author: wrichards@mit.edu*

Received November 20, 2008; revised February 7, 2009; accepted February 9, 2009;
posted February 27, 2009 (Doc. ID 94954); published April 7, 2009

Unlike the Metelli monochrome transparencies, when overlays and their backgrounds have chromatic content, the inferred surface colors may not always be physically realizable, and are in some sense "imaginary." In these cases, the inferred chromatic transmittance or reflectance of the overlay lies outside the RGB spectral boundaries. Using the classical Metelli configuration, we demonstrate this illusion and briefly explore some of its attributes. Some observer differences in perceiving transparencies are also highlighted. These results show that the perception of transparency is much more complex than conventionally envisioned. © 2009 Optical Society of America

OCIS codes: 330.0330, 330.5020, 330.5510, 330.7310, 350.2450, 290.7050.

1. INTRODUCTION

Color is an important perceptual attribute of surfaces. Perhaps the most common way to identify perceived color is by way of an atlas, such as the Munsell Atlas. Under standard illumination, the tokens in an atlas can be mapped into a triple of RGB (tristimulus) values in the CIE system. These triples specify completely the gamut of all colors observed for Lambertian surfaces seen under the standard illuminant and occupy what is designated as the color solid [1]. If an RGB tristimulus value lies outside the color solid for the illuminant, then that stimulus is physically unrealizable, or, in some sense "imaginary."

Definition: An unrealizable surface color is represented by tristimulus values that lie outside the boundaries of the color solid, implying a nonphysical, Lambertian spectral reflectance.

To illustrate, P and Q in Fig. 1 are seen by most observers as colors of a single homogeneous transparent surface that overlays two opaque surfaces A and B of different reflectance. In fact, if the physics is modeled using either the Metelli or the Kubelka–Munk formulation, then the perceptual interpretation leads to unrealizable RGB tristimulus values. This is illustrated in the left panel of Fig. 2 using the RGB unit cube to approximate the boundaries of the color solid [2]. This kind of violation was first noted in the late 1970s [3].

In the Metelli model, the inferred color of a transparent surface that overlays a background is the composite of two parameters: the spectral reflectance α_λ and the transmittance τ_λ of the overlay. Both must lie in the interval [0, 1]. Metelli [4–6] proposed a simple linear model where the fraction τ_λ of the light from the background was transmitted through the overlay, and the remaining fraction $(1-\tau_\lambda)$ was reflected off the overlay. (This model may be regarded as an approximation to the Kubelka–Munk formulation [7]). Because Metelli's model simply adds some fraction of light from the background to that reflected off the overlay, the chromaticity of P must lie on a line from the inferred RGB values of the overlay to the RGB values of its background, namely A, and similarly for B and Q.

This condition is illustrated in a depiction of an RGB chromaticity plot in the right panel of Fig. 2. The intersection V of these two loci is the expected observed chromaticity, which in this case lies within the spectral boundary and hence is physically plausible. In contrast, the left panel shows the condition of particular interest to us. As mentioned earlier, here the Metelli model is violated because the RGB values of the overlay lead to chromaticities that have a negative B value, with point V lying outside the RGB triangle and even beyond the spectral locus. This is physically unrealizable [1,3].

In our experiments, we focus on the inferred spectral reflectances α_λ and transmittances τ_λ of the perceived transparent overlays, rather than the perceived color of the overlay. To deduce the inferred α_λ and τ_λ values from the subject's settings of RGB tristimulus values, we simply apply Metelli's model [4,7]:

If P_λ, Q_λ are the two regions of the overlay, and if the two background regions are A_λ, B_λ as shown in Fig. 1, then the tristimulus values of the observed colors will satisfy

$$P_\lambda = \tau_\lambda A_\lambda + (1-\tau_\lambda)\alpha_\lambda, \tag{1a}$$

$$Q_\lambda = \tau_\lambda B_\lambda + (1-\tau_\lambda)\alpha_\lambda. \tag{1b}$$

These conditions lead to the following two constraints on relations between the observed components of the background A_λ, B_λ and the overlay P_λ, Q_λ:

$$(0 \leqslant \tau_\lambda \leqslant 1) \Rightarrow 0 \leqslant (P_\lambda - Q_\lambda)/(A_\lambda - B_\lambda) \leqslant 1, \tag{2}$$

$$(0 \leqslant \alpha_\lambda \leqslant 1) \Rightarrow 0 \leqslant (-P_\lambda B_\lambda + A_\lambda Q_\lambda)/(A_\lambda - B_\lambda - P_\lambda + Q_\lambda) \leqslant 1. \tag{3}$$

Henceforth we will eliminate the λ subscripts, it being understood that conditions (2) and (3) will be checked for all

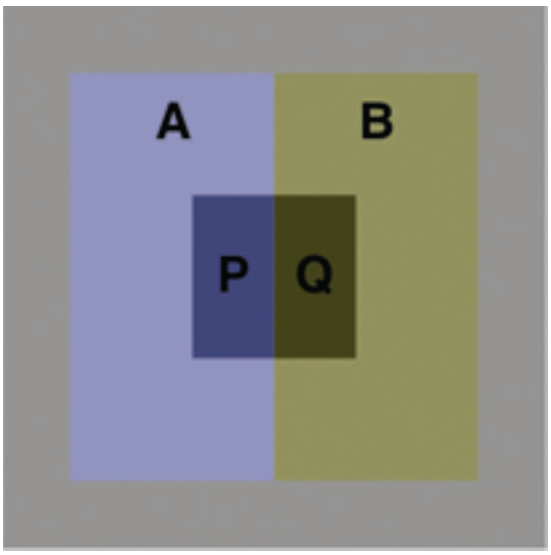

Fig. 1. Example transparency. The RGB values are: A= ={0.50,0.50,0.70}; B= ={0.50,0.50,0.30}; P= ={0.20,0.20,0.40) and Q= ={0.20,0.20,0.05}. Using Metelli Eqs. (1), a reflectance and transmittance of the overlay can be calculated for each RGB tristimulus value. For this example, the inferred reflectance and transmittance for the B tristimulus values were, respectively, −0.63 and 0.73. The negative value indicates a Metelli violation requiring an unrealizable or "imaginary" spectral surface color (see Fig. 2).

three RGB tristimulus values used to generate the displays. These formulas completely describe the physics (but see Appendix B for qualifiers).

2. METHODS

Displays similar to Fig. 1 were generated on a G4 eMac computer. The x, y chromaticities were [{0.64, 0.33}, {0.28, 0.60}, {0.15, 0.073}] with maximum screen luminance of 145 cd/m^2 as calibrated by LaCIE Blue eye and Monaco Optix instruments. The gamma was set at 1.0, and the illuminant was modeled as D65 (0.312, 0.329). The overall display subtended 18×18 cm and created a neutral gray background of luminance 48 cd/m^2. Superimposed on this background were the two adjacent panels A and B, each 7.5×15 cm. On top of these panels was a 4×4 cm overlay split vertically into halves to create panels P and Q. The typical viewing distance was 60 cm. (This was not a critical parameter).

At the bottom of the display was a slider that could be moved by the subject to adjust RGB values. In pilot studies, these values were set for each panel, enabling us to explore a wide range of conditions. During this series we observed several subjects who would accept partial transparencies when only one panel satisfied the Metelli conditions [8–14]. Hence, to avoid independent settings for P and Q, we linked the RGB values of the two halves of the overlay.

Our setup is clarified in Fig. 3, which is part of a planar section in RGB space. This plane is defined by the RGB values of A, B, and the anchor point *max-PQ*. This last point is the most extreme RGB value for P,Q for the chosen task. Given points A,B we then located their midpoint C. Now a line L_{pq} joining *max-PQ* with C (*mid-AB*) can be calculated. Twenty to thirty-five uniformly spaced RGB positions along the line L_{pq} were chosen, the number depending upon the experiment, ranging from *max-PQ* to *min-PQ* as illustrated in Fig. 3. From each of these positions, the two sets of RGB values were calculated, one for P and the other for Q at an orientation parallel to AB. These values of P and Q were yoked to depart symmetrically from the line L_{pq}. The extent of the departure from L_{pq} was controlled by the subject using a slider visible at the bottom of the display. Hence, if the *mid-PQ* position were set at the position C on the line L_{pq}, the extreme PQ settings would be A and B. A similar procedure was used at all other points along line L_{pq}. Hence, at each of these points, the chromaticities of P and Q were pulled apart until the subject failed to see the PQ overlay as transparent. (Note that unlike the anchor point *max-PQ*, over most of the interior region of the parallelogram, it is possible to pull P,Q apart so their RGB positions lie outside the parallelogram). The P–Q separation was then reduced until the percept of transparency reappeared, and this setting was entered into a data file as the transparency limit for that trial. The result is a set of PQ values that construct (curved) loci analogous to the AV and BV rays shown in Fig. 2. These loci were stored as the responses.

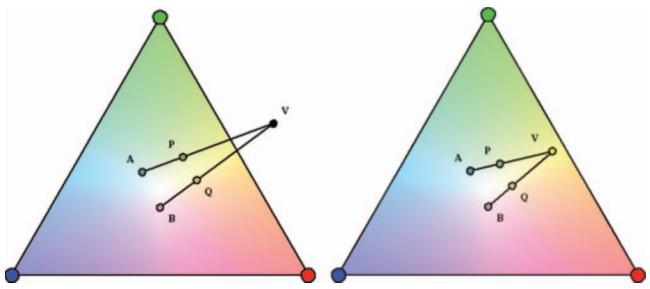

Fig. 2. Slice at the RGB color space showing a violation of the Metelli conditions (left) and another example that is physically realizable (right).

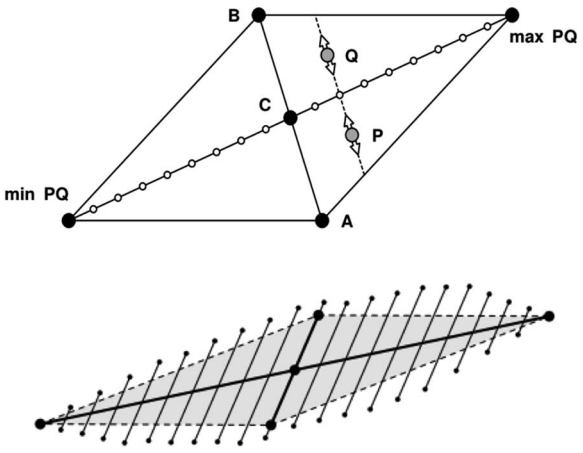

Fig. 3. Depiction of the experimental conditions. The parallelogram is part of a plane in RGB space defined by the points, A, B, and an anchor point *max-PQ*. Points are chosen along the line through C joining *max-PQ* and *min-PQ*. The boundary of the parallelogram indicates the limiting PQ settings for the Metelli conditions. In the lower panel, we show averaged settings for task 8 (Fig. 4). Note that observers accept settings that lie outside the parallelogram.

During each trial, there was also a calculation that determined whether any of the RGB beam values were inadvertently being frozen at their maximum levels. A signal light indicated when such clipping occurred, and these settings were replaced by the limiting values just inside the clipping.

3. ANALYSIS

A. Metelli Limits

The response files contained the set of RGB values for P and Q, as well as the inferred reflectance α_λ and transmittance τ_λ, as calculated from Eqs (1). (Summaries are given in Appendix A, showing the RGB values for A,B and P,Q for some of the more important violations). To simplify the analysis, the data for each trial were typically plotted in rank order on the [0, 1] interval with *min-PQ*=0 at the left end of the scale and *max-PQ*=1 at the right end. For most cases, these extreme values for transmittance and reflectance are pinned at 0 or 1 by this construction, and are the expected limiting values. Figure 4 shows example plots for one condition where only the B tristimulus values were varied by the subject. (The RGB parameters were $A=\{0.5,0.5,0.7\}$, $B=\{0.5,0.5,0.3\}$, and *max-PQ*=$\{1,1,1\}$, as shown in row 1 of Table 1 in Appendix A). The upper plot gives the value of the inferred transmittance of the overlay needed to satisfy the Metelli condition, while the lower plot shows the result for inferred reflectance. Note there is a regular pattern with almost half the points requiring nonphysical values for either transmittance or reflectance. However, the regions of the violations are different for each, as will be discussed shortly.

Although we did not systematically record perceived chromatic aspects of the overlay, there was general consensus about achromatic effects, which fell into three different regions: blackish, grayish, and whitish. These are indicated in Fig. 4 by vertical dashed lines L, M, and H, which are mnemonics for "lower," "middle," and "high" values for *PQ*. Slice M corresponds to the trial position where the *PQ* overlay has RGB values midway between those for A and B. Hence by adjustment of the slider, P and Q can, respectively, match A and B. Ideally, we expect that at *mid-PQ* the extreme settings should be A and B with $\tau_\lambda=1.0$ and the inferred reflectance α_λ equal to the average of A and B. However, this condition is an obvious singularity. Although the extremes for τ_λ are typically greater than one in this region, we sometimes find a dip in transmittance back toward 1 near *mid-PQ*=0.5 (line M in Fig. 4).

A second, and more interesting type of singularity appears near the lower and higher regions of the reflectance calculation indicated by the lines L and H in Fig. 4. These lines correspond to *PQ* values of 1/3 and 2/3. Note that to the left of L and to the right of H, we have violations in α_λ, with high variance near L and H. Both slices correspond to a change in the sign relationships between the denominator and the numerator of Eq. (3). For the illustrative example, the value of $(A-B)$ is fixed over all trials, but the $P-Q$ difference increases as the overlay changes from dark tones, through gray, to white. Near both L and H these differences are numerically similar to the $A-B$ difference. Data points near these singularities had high variance, and values that exceeded 1.5 or were less than −0.7 are plotted on the panel boundary.

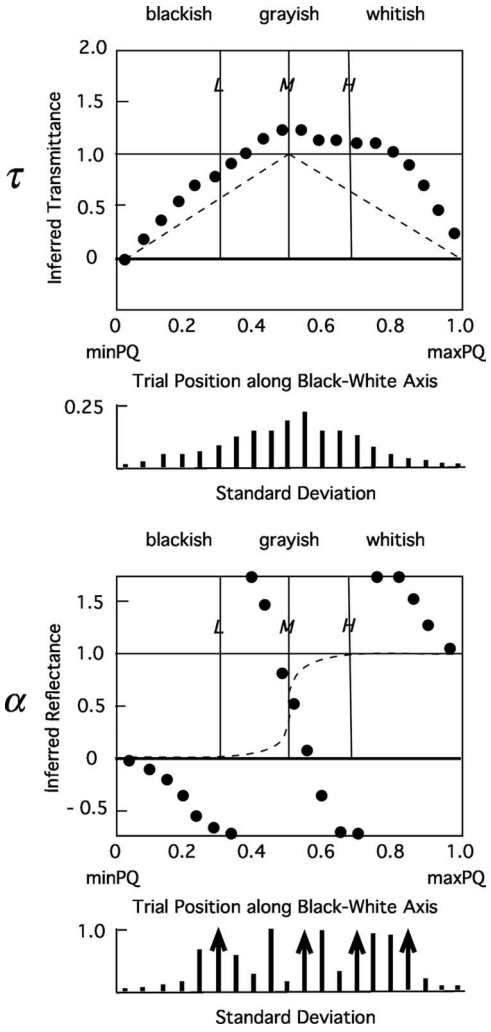

Fig. 4. Averaged values of transmittance τ_λ (top) and reflectance α_λ (lower) for the upper bounds of transparency settings of eight subjects for task 8 (see Table 1 in Appendix A). The dashed curves indicate values if both of Metelli's conditions were met at the same time (the ideal step function for the lower panel has been smoothed slightly). The L and H vertical lines give approximate boundaries for grayish tones to the overlay (below L, very dark; above H, very light). Note that although reflectance is mostly within the [0,1] interval over the grayish range, most of the transmittances exceed one. Similarly, the reverse is true outside this gray interval. (Points greater than 1.5 or less than −0.7 are plotted on the upper and lower boundaries of the panel. Arrows indicate very large values for standard deviations that exceeded the range indicated on the left).

One might argue that both the L and H violations are simply due to noise in the observer's settings, and hence are not significant. However, the pattern of three negatively sloped loci about the L and H singularities reveal an underlying regularity that clearly is not just noise. Furthermore, note that if we consider both transmittance and reflectance together, the Metelli violations occur over the full range explored, not just in the L and H regions. The reflectance violations α_λ occur when the overlay has a blackish or whitish tint, whereas the transmittance τ_λ violations occur when the overlay appears grayish. Clearly, there is a real effect here.

Of passing interest are the loci for both α_λ and τ_λ if they are simultaneously satisfied and follow the boundary of the *A*, *max-PQ*, *B*, *min-PQ* parallelogram illustrated in Fig. 2. The dashed curves in Fig. 4 show this constraint, relaxed slightly for α_λ. For transmittance, all points lie on a triangle with the reflectance of 1 at *mid-PQ*=0.5 and are zero at both *max*- and *min-PQ*. For reflectance, the limiting locus is a step from 0 to 1 at *mid-PQ*. In Fig. 4 this locus is rounded to create an ogive, which better reflects plausible observer settings.

B. Kubelka–Munk Limits

The Metelli model assumes that the fraction τ_λ of light coming off the background is transmitted through the overlay without internal scatter. A more realistic physical model is to include effects of all light scattered internally off the opaque particles of the overlay. In this vein there have been several analyses of optical conditions, such as haze or fog, or filters with internal reflections, that indicate the Metelli model, although very simple, is a good approximation for other transparency effects [15–20]. To add to this list, we have calculated the equations for inferring physical absorbance and turbitity transmittances, according to the Kubelka–Munk model [1,7,21,22]. Appendix A includes the results of these calculations for some of our trials. As others have found before us, the limiting conditions for the more physically realistic models were rather similar to Metelli's. Hence when a Metelli violation occurred, typically that setting also violated the Kubelka–Munk model (see also [23]). The intuitive explanation for the similar results is that sign shifts in the contrast difference between *P* and *Q* and *A* and *B* usually do not survive either model.

4. RESULTS: CONDITIONS FOR UNREALIZABLE COLORS

Perceptual violations of any physical model can be the result of an inadequate model, or alternatively, a failure in perceptual inference, or both [24]. A few simple examples, together with informal observations, show that most of the violations we observe are the result of nonveridical perceptual inferences as well as inadequate physical models for configurations of opaque and turbid layers.

A. Independence of *L*,*M*,*S* Chromatic Channels

Models for transparency, such as Metelli's, that ignore fluorescence imply that light from any spectral region will act independently of light from another spectral region. In contrast, an observer's long-, middle-, and short-wave chromatic channels (*L*,*M*,*S*) may interact, such as when they are combined for brightness estimates, or in a color-opponent representation. To test for the independence of the *L*,*M*,*S* channels, let us keep the B tristimulus values of *A* and *B* as before in Fig. 4, but shift the R and/or G tristimulus values of *A* and *B* either toward the red or the green. Similarly, we shift the *max-PQ* value (i.e., the original {1, 1, 1} values) by a similar amount. (In the R-shifted case the new *max-PQ* values will be {1, 0.7, 0.7} and the upper limit for the B tristimulus value will be 0.7). Such a lateral shift in the RGB space does not affect the conditions on τ_λ and adds a mild constant to α_λ. Hence the result shown in the upper panel of Fig. 4 should be unchanged, whereas the lower panel will change by a vertical shift. [This claim is easily checked by referring to Eqs. (2) and (3)].

Five subjects previously run on task 8 were run on this new task 21 (see Appendix A). Although the results of some of these observers exhibited three negatively sloped regions as seen on the earlier task (i.e., the pattern in Fig. 4), the averaged data for all of the subjects used for task 21 had extremely high variance. This was most pronounced on the inferred reflectance. Further inspection of individual data revealed that the high variance findings resulted from averaging over two quite distinctive patterns. These individual differences are exhibited in Fig. 5.

Two of the five subjects had patterns for inferred transmittance and reflectance similar to that of Fig. 4, with inverted U-shaped loci for transmittance τ_λ and negatively sloped loci for reflectance α_λ. Their data are shown on the left two panels of Fig. 5. For these subjects, the R-shift manipulation thus had little effect on the B tristimulus settings other than the expected truncation above 0.7 on the *PQ* axis where no data points could be collected. We conclude that for these observers there was little or no interaction between the *L*,*M*,*S* chromatic channels.

In contrast, however, three of the five subjects had changes that were not expected. As shown in the right panels of Fig. 5, these new patterns appeared in both the inferred transmittance and especially in the inferred reflectance. For these observers, the transmittance (top right) now falls within the acceptable 0–1 interval, as do most of the reflectance values (lower right), excepting where the overlay has a very dark color (i.e., to the left of the vertical line L). Excepting this lower quarter of the range, the inferred reflectance increases almost monotonically to reach 1 at the extreme *P*,*Q* anchor point. This is a dramatic change from Fig. 4 and shows that for some observers, there can be strong interactions between the long-wave *L* channel or the middle-wave *M* channel and the short-wave *S* chromatic channel.

B. Role of Achromatic Axis

From the results of Fig. 5, which were based on a red shift from an achromatic locus, one might expect that for some observers, a blue-green shift in the opposite direction might again lead to two or more varieties of results. Hence task 13 was introduced to shift the mean of *min-PQ* and *max-PQ* toward the green (see Appendix A for settings). Four observers previously run on task 21 (Fig. 5) were run on task 13. One of these was significantly different from the other three, with patterns resembling task 8. For the remaining three observers, the shift of the display toward the green resulted in much less severe violations. Figure 6 shows their averaged results. On the top are the inferred transmittances. These data are the same for all three RGB tristimulus measurements. On the bottom, the solid circles show the Metelli reflectances calculated from the G tristimulus measurements, while the open circles show reflectances calculated from the B tristimulus values. Note the very compressed dynamic range for the latter, whereas the former shows an almost linear progression in α_λ. However, the transmittance inferred from all three tristimulus values (top),

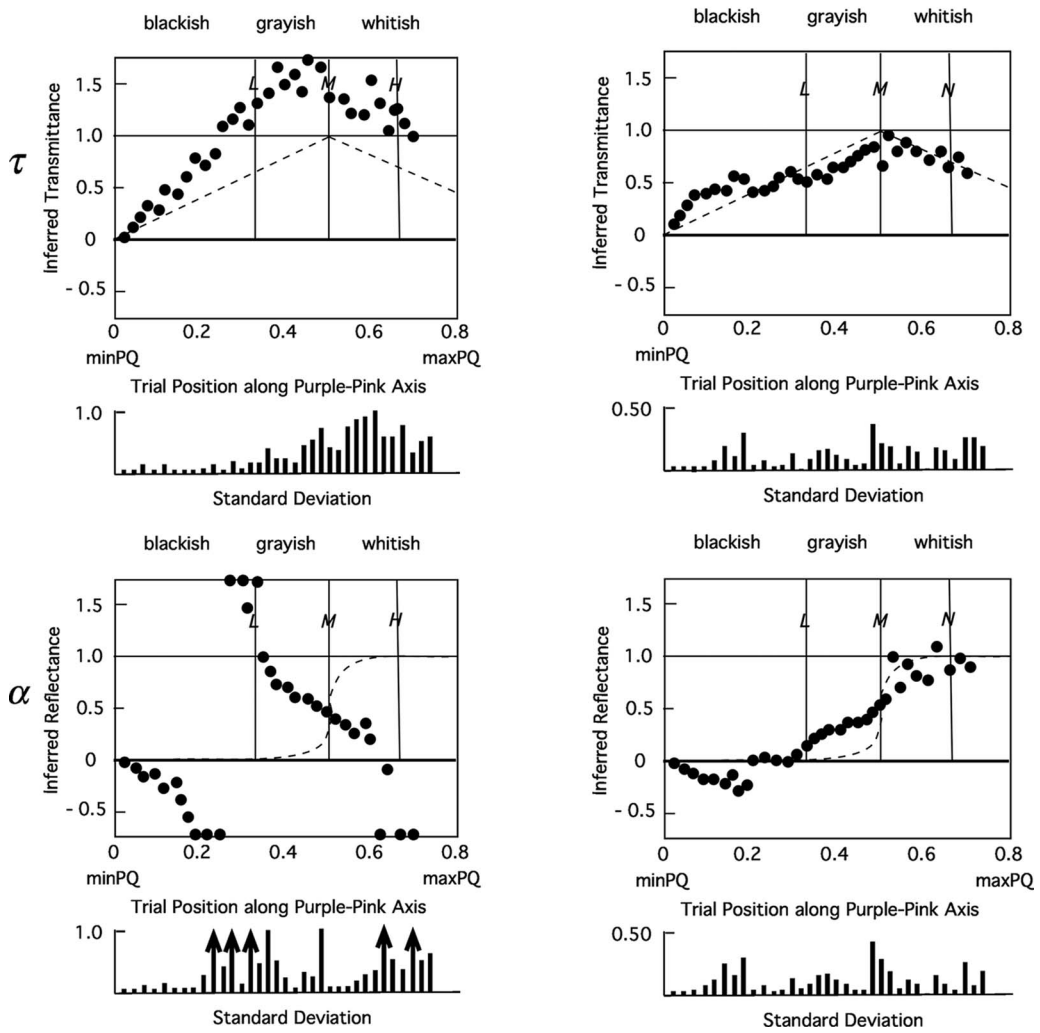

Fig. 5. Inferred transmittance (top) and reflectance (bottom) for task 21, where the *PQ* loci are shifted to the red. The left two panels are data from two subjects, the right panels are data from three subjects, all of whom provided similar data for task 8 (Fig. 4). The *PQ* values of the overlay vary from pinkish to dark purple, with *max-PQ*={1,0.7,0.7}. The background panels are *A*={0.8,0.5,0.7}, *B*={0.8,0.5,0.3}. See Appendix A for further details.

shows the characteristic triangular form, lying well within the Metelli limits for this class of observer.

The most significant difference between the conditions of Figs. 5 and 6 is that in the first case, the *PQ* locus is roughly parallel to the achromatic (black–white) axis, whereas in the second case the *PQ* axis is tilted to run from a dark purple through a greenish gray to end in a very light green. (Using the Munsell notation [1], *A* is a violet (5PB5/8), whereas *B* is a yellow-green (7GY7/7)). The consequence of the second manipulation is to reduce the perceptible achromatic tint (e.g., blackish, grayish, whitish). This observation, in addition to the markedly reduced violations seen for the same three subjects for the Fig. 5 (right) condition, suggests to us that an achromatic channel plays a role in the inference of transparency—at least for some observers.

C. Perceived Depth of Overlay

Laboratory setups have reduced constraints as compared with real-world conditions. A consequence is that the conventional Metelli configuration illustrated in Fig. 1 and used here has a very large number of categorically different interpretations [9,23–29]. For example, as mentioned, either *P* or *Q* may appear transparent, but not both (we instructed our subjects to consider this a violation). But more extreme, *PQ* can appear as a surface behind a window in *A* and *B*. Surprisingly, many of our subjects could not see—or NEVER saw—this condition, whereas others rejected this percept as an acceptable transparency (because we specifically stated that *PQ* were to appear as an overlay). One of our eight subjects was known to be stereo-anomalous [30,31], with reduced ability to process uncrossed disparities. Extensive studies with this subject confirmed that the extreme violations of the Metelli condition, including those for Fig. 5 (left), typically occurred when others rejected *PQ* as lying behind, not in front of *AB*.

We also note that some observers can key in on different color channels, and this attention variable can affect the results. For example, if those channels become the dominant attribute of a surface behind the window, this percept can be ignored (both JJK and WR could easily

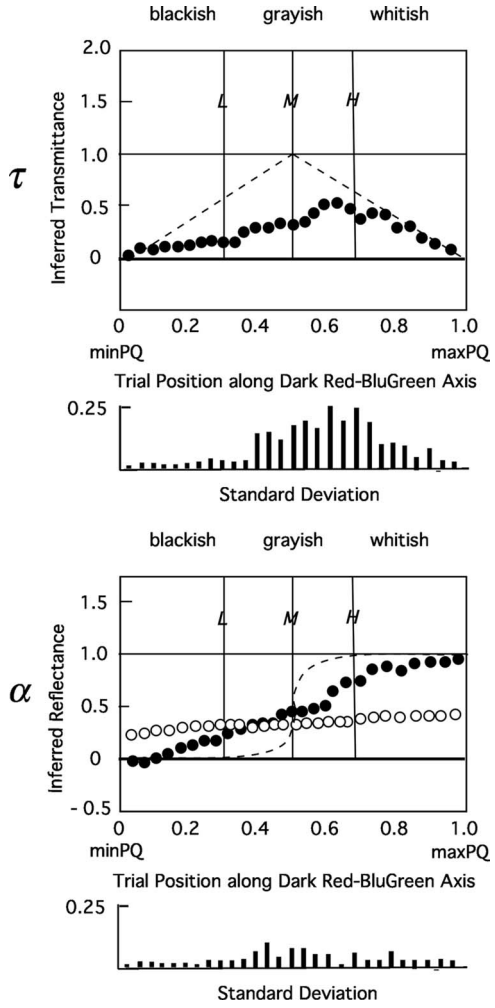

Fig. 6. Inferred transmittance (top) and reflectance (bottom) for task 13 for three subjects used also for task 21 (right panels of Fig. 5). For task 13 the *PQ* loci are shifted away from the achromatic locus to the green. The *PQ* values of the overlaid region vary from light blue-green (5BG8/5) to red-purple (2.5RP3/8), moving through a greenish gray. *max-PQ*={0.4,1,0.4}. The background panels are A={0.2,0.3,0.7}, B={0.5,1,0.01}. The transmittances for all three channels are the same; the open circles show the compressed reflectance values inferred from the B tristimulus values; the solid circles show those inferred from the G tristimulus values. See Appendix A and text for further detail.

perform this manipulation). However, if the discrimination is absent, such as in a color-anomalous observer, for example, that channel may contribute to the inference of an overlay, where it would otherwise be rejected. This attention factor further increases the complexity of the transparency percept and must be considered when counting the number of categorically different transparency interpretations for the observed *PQ* versus *AB* depth relations for each colored layer.

5. DISCUSSION

Although the failure of simple physics-based models to account for transparency perception have been noted before [3,11,24,32–34], our observations document some new and important characteristics. First, not previously noted, there is an unusual, non-monotonic pattern to the inferred reflectance violations, as shown especially in Fig. 4. However, as shown by Fig. 5, for some conditions and some observers, this pattern of inferred reflectance can become monotonic over almost all of the range. This difference between observers appears to be *categorical*; hence future studies should not treat all observers as belonging to only one category. Third, although we know that violations occur in either inferred transmittance or reflectance, both types of violations typically do not occur simultaneously. Finally, as noted by others [13,26,35–38], the achromatic axis appears to play a special role in perceptual transparency.

The failure of Metelli-like models is most obvious when the perceptual inference of transparency leads to colors that are nonrealizable and are, in that sense, imaginary (e.g., the depiction in Fig. 2). Why observers accept certain nonphysical conditions as transparent is not entirely clear. One explanation is to note that, unlike achromatic Metelli configurations, the perception of colored transparency will involve several chromatic channels in the visual system. Hence a simple hypothesis is that if one (perhaps more) of these channels has (have) a violation but a weak signal, and the remaining channels have strong signals and satisfy the Metelli conditions, then the observer will accept the overlay as transparent. Indeed, many of our results are consistent with a version of this hypothesis. For example, if observers differ in the proportion of active L, M, S channels that exhibit violations, this hypothesis could explain the observer differences in task 21 shown in Fig. 5. (See also Appendix B).

A related possibility is that observers might require different thresholds for what they consider acceptable signals in each of the L, M, S channels. The effect of such a threshold will become very apparent if the contrast of the display is reduced. Then violations are more likely because the judgments are difficult, with the *PQ* separation much more difficult to notice. On the other hand, in the opposite case where the signals of all channels are raised to comparable levels, violations are expected to be much less frequent, especially if the display is roughly equiluminant, for then the contrasts between regions in the L or M channels will be weak, but the short-wave S channel can be boosted without affecting equiluminance. In this case the violations are minimal and are confined to the *PQ* extremes.

The hypothesis that strong signals in L, M, S channels satisfying the Metelli conditions will dominate the violations in chromatic channels with weaker signals raises the question of how many channels are sufficient to produce the appearance of transparency. If percepts are based on the L, M, S channels, then we expect only three channels to be in play. However, if transparency perception is based on an opponent-color system, then the channels take a different form, such as the opponent Y-B, R-G, K-W. In this formulation, the achromatic K-W channel plays an explicit role, which is not the case for L, M, S. In addition, excepting the equiluminance case, Appendix C shows that the Metelli conditions cannot be verified for Y-B and R-G. But it can be shown that if Metelli violations occur in any one of the L, M, S channels, then there is a 99% certainty that there is a violation in the luminance or achromatic channel. This means that in almost all cases,

Table 1. Experimental Parameters and Violations

Task No.	*Max-PQ*	{*A*,*B*}	Pos. No.	{τ_λ-α_λ}	Metelli Violation (*PQ*)	Comment
8	{1.0, 1.0, 1.0}	{0.5, 0.5, 0.7}	[5]	{0.7, −0.7}	{0.20, 0.20, 0.35}	
		{0.5, 0.5, 0.3}			{0.20, 0.20, 0.05}	K-M violation
			[10]	{1.2, 0.7}	{0.50, 0.50, 0.70}	
					{0.50, 0.50, 0.20}	K-M violation
			[17]	{0.9, 4.4}	{0.80, 0.80, 0.98}	
					{0.80, 0.80, 0.61}	K-M violation
13	{0.4, 1.0, 0.4}	{0.2, 0.3, 0.7}	[2]	{0.13, −0.03}	{0.24, 0.01, 0.33}	
		{0.5, 1.0, 0.01}			{0.28, 0.10, 0.23}	Minor G violation
20	{0.8, 1.0, 1.0}	{0.2, 0.5, 0.7}	[6]	{1.1, −0.5}	{0.32, 0.6, 0.82}	
		{0.2, 0.5, 0.3}			{0.32, 0.6, 0.38}	K-M violation
			[7]	{1.05, −2.5}	{0.38, 0.65, 0.86}	
					{0.38, 0.65, 0.44}	K-M violation
21	{1.0, 0.7, 0.7}	{0.8, 0.5, 0.7}	[8]	{0.75, −0.83}	{0.46, 0.16, 0.31}	Redshifted task 8
		{0.8, 0.5, 0. 3}			{0.46, 0.16,.012}	
31	{1.0, 1.0, 1.0}	{0.3, 0.7, 0.7}	[18]	{0.7, 1.7}	{0.71, 0.99, 0.99}	K-M violation
		{0.7, 0.3, 0.3}			{0.99, 0.71, 0.71}	
32	{0.7, 0.7, 1.0}	{0.3, 0.7, 1.0}	[24]	{1.05, 1.1}	{0.27, 0.69, 0.99}	Blue shift 31
		{0.7, 0.3, 0.6}			{0.69, 0.27, 0.56}	One minor violation

for the opponent-color system *only* the achromatic channel needs to be checked for Metelli violations.

Let us suppose, however, that observers used an opponent process scheme to judge transparencies (and hence did not ignore the chromatic Y-B, R-G channels). In this case, violations can be introduced (such as in task 8). For example, observers may not always ignore the Y-B, R-G channels and may add chromatic content to the display to create a hint of the background in the overlay [11,24]. Then violations resulting from adding chromatic content will have the greatest effect in the presence of strong achromatic signals, namely, when the percept is of a black to dark gray or the complementary percept of light gray to white, as seen in Figs. 4 and 5.

Curiously, when the display is equiluminant, adding tints of the background to the overlay can lead to physically plausible transparencies using an opponent-process scheme. First, note that in this case, the achromatic channel conveys no significant information about the overlay. Hence the Metelli transparency can be decided on the basis of whichever opponent channel carries the significant structural information. As shown in Appendix D, the condition is that the opponent channels should have equal sign and that the contrast in the overlay should be lower than that in the background.

In sum, although we favor the hypothesis that observers use an opponent-process scheme for judging transparency, we have no conclusive proof that this is the case. The striking differences among observers also presents a problem: Do some observers rely more on the achromatic channels than others? Or are all observers using an opponent-process scheme, with some invoking the chromatic channels in nonequiluminant conditions when others do not?

Our final comment addresses again the main claim, namely, that violations of the Metelli conditions (or the Kubelka–Munk model [21]) can easily be created in chromatic displays. This does not imply that most inferences about transparency in the real world will be flawed. First, many additional constraints come into play, and these typically augment the reduced conditions created in the laboratory. Second, perhaps more important, is that the violations reported here assume the Metelli model of a homogeneous turbid overlay. However, analogous situations appear in the natural world that are created in other ways. For example, consider the occluding contour of neighboring surfaces where a shadow is cast across the boundary. This "x-junction" has the same form as the junction formed between the *P*, *Q*, *A*, *B* regions of Fig. 1 and certainly plays a major role [32,35]. But the model will be quite different because in this case the scattering is absent, like a clear overlay without turbidity.

Another common configuration that has the same appearance as the panels in Fig. 1 would be if the interior square is a hole, with surfaces *P*, *Q* lying behind *A*, *B*. Then again, the Metelli model is not appropriate. In fact there are four conditions of this kind that correspond to the placement of the plane of the transparent surface [23]. In our experiments, although many observers consistently saw the *PQ* panels as in front of *AB*; others observed cases where *PQ* appeared as a hazy film behind *AB*. Their settings may have been appropriate for this interpretation. Hence depth assertions also can influence judgments of transparency and may help distinguish between related phenomena such as translucency, fluorescence, or shadows [29]. Simply put, there are a variety of physical phenomena with many distinctive underlying parameters; we cannot expect a system with limited, reduced stimuli to categorize all these phenomena reliably. Understanding perceptual transparency in a real-world setting will require a much more complex model than Metelli's, namely, one that considers the gestalt associated with a host of possible physical interpretations that include spatial configurations, their depth relationships, and how they are illuminated, as well as the chromatic content of the display [23].

APPENDIX A: EXPERIMENTAL PARAMETERS AND VIOLATIONS

The task number, max-PQ, and $\{A,B\}$ settings are shown in the first three columns of Table 1. (Note that the latter two values fully specify the task). In the remaining columns, we list some representative violations, but not necessarily the extremes for α_λ and/or τ_λ. For example, from the plots of Fig. 4, we picked trial 10 for transmittance, and trials 5 and 17 for reflectance for the blue channel.

APPENDIX B: INDEPENDENCE OF SPECTRAL SUBCHANNELS

Consider a system made up of two nonoverlapping spectral subchannels. Suppose the Metelli transparency conditions are checked for each channel separately. Moreover, suppose these conditions are also checked for the superchannel formed by merging the two subchannels. This might happen in a system with two spectrally selective channels in which an "achromatic channel" were formed at a secondary stage, the subchannels being of a primary (retinal) stage. Then an important question is: If the Metelli conditions are satisfied at the subchannel stage, can they ever be violated at the secondary stage, that is for the superchannel?

The answer would be immediate if the Metelli conditions were linear [7]. For instance a "luminance" signal could be computed at the subchannels (e.g., L, M) and the luminance computed for the superchannel would simply be the sum of these two luminances. Thus equality of luminance could be checked either at the primary level (adding the two outcomes) or at the secondary level; it would make no difference. In the Metelli transparency case, which is nonlinear, it is feasible that the conditions are satisfied in both subchannels, but are violated for the superchannel. Although the Metelli constraints are only mildly nonlinear (the dividing surfaces in parameter space being either planar or ruled surfaces) this condition still has to be analyzed.

Consider again the Metelli conditions for transparency in the case of two background areas A and B that appear as two different colors behind a single transparent overlay P and Q, where P is A as seen through the overlay, and Q is B as seen through the overlay (i.e., Fig. 1). The condition is

$$\begin{aligned} F(A,B;P,Q) = (((P > Q) \wedge (A > B)) \wedge ((((Q + A + PB) \\ > (P + QA + B)) \wedge (P > A)) \vee ((P < A) \\ \wedge (PB < QA)))) \vee ((P < Q) \wedge (A < B) \\ \wedge (((PB > QA) \wedge (P < A)) \vee ((P < A) \\ \wedge (Q + A + PB) < (AB + QA + B))))). \end{aligned} \quad \text{(B1)}$$

For the two subbands 1, 2 we write

$$C_1 = F(A_1,B_1;P_1,Q_1),$$

$$C_2 = F(A_2,B_2;P_2,Q_2), \quad \text{(B2)}$$

and for the superchannel

$$C_{1+2} = F\left(\frac{(A_1+A_2)}{2},\frac{(B_1+B_2)}{2};\frac{(P_1+P_2)}{2},\frac{(Q_1+Q_2)}{2}\right), \quad \text{(B3)}$$

where we divide by two to keep the values within the [0, 1] range. Then

$$H = (C_1 \wedge C_2) \wedge \neg C_{1+2} \quad \text{(B4)}$$

expresses the violation of the Metelli transparency condition for the superchannel when the conditions are satisfied in both subchannels. Algebraic simplification (done via Mathematica) yields a very long expression (16 lines) that conceivably might still be identically TRUE. In order to decide the issue we evaluated the expression for random values of the parameters, where A, B, P, and Q for either channel were drawn from a uniform distribution on [0, 1].

We find that in about 1% of the cases the expression evaluates to TRUE, in 99% of the cases to FALSE.

Thus when the Metelli conditions are satisfied in the subchannels there is indeed no *guarantee* that they might not be violated in the superchannel, though this will happen only in *rare cases*. For the purposes of the present work it is safe to ignore such rare occurrences.

In case Metelli is not violated in the superchannel, it is still possible that there is a violation in one or both of the subchannels. Consider the sequence {1st subchannel, 2nd subchannel, superchannel}. Let T stand for TRUE (i.e., Metelli constraints satisfied), F for FALSE (Metelli constraints violated). Then we find from a simulation of 10^5 cases the following estimates of frequencies of occurrence:

FFF	58.6%
FFT, TFF, FTF	10.6%
FTT, TFT	3.34%
TTF	0.896%
TTT	1.90%

All combinations occur, though with very different frequencies. Apparently, acceptance of transparency in the superchannel by no means implies absence of violation in the subchannels.

Note that the trichromatic case is not essentially different from the dichromatic case considered here.

APPENDIX C: METELLI CONDITIONS IN AN OPPONENT COLOR SYSTEM

Consider the simple case of a dichromatic opponent system. For convenience, relabel the two spectral subband channels X, Y and propose two superband channels U, which is a superposition channel, and V, which is a difference channel. Then U and V are encoded as U=(X+Y)/2, that is the "achromatic channel," and V=(X−Y)/2, that is the "opponent channel." When X, Y are on [0,1], then U, V are again in [0,1], whereas the opponent signals vary on [−1/2, +1/2].

We write the background areas A and B as (K+L)/2 and (K−L)/2, respectively, where K denotes an "achromatic" and L an "opponent" channel. Likewise, we write

the areas P and Q (that are the backgrounds A and B as seen through the transparent overlay) as $(S+T)/2$ and $(S-T)/2$, respectively, where S denotes an "achromatic" and T an "opponent" channel. The Metelli condition can thus be expressed as (see Appendix B)

$$F\left(\frac{K+L}{2}, \frac{K-L}{2}; \frac{S+T}{2}, \frac{S-T}{2}\right). \tag{C1}$$

This inevitably leads to a rather complicated expression. However, it can be simplified considerably, and without sacrificing generality, by considering suitable special cases. Consider the case $A>B$. It is still general, for if $A<B$ then we simply mirror reflect the Metelli configuration. Now $A>B$ implies $P>Q$ when Metelli transparency is to be possible, so we may assume both $A>B$ and $P>Q$ here. Then the expression simplifies to $(KT<LS)$, which we prefer to write as

$$\frac{L}{K} > \frac{T}{S}, \tag{C2}$$

in which ratios of the opponent to the corresponding achromatic channels are compared. But this implies that the Metelli transparency conditions cannot be expressed in a form

$$G(K,S) \wedge H(L,T), \tag{C3}$$

where $G(K,S)$ is a constraint in terms of the achromatic and $H(L,T)$ an independent constraint in terms of the chromatic signals.

Thus one cannot have a system that checks for Metelli consistency in independent achromatic and opponent channels and subsequently combines the results by a logical AND. In order to check Metelli transparency one needs to consider the achromatic and opponent channels *simultaneously*, essentially backtransforming to the primary intensity (nonopponent) channels.

To summarize, for the case of a true opponent system one expects Metelli transparency to be a function of the achromatic channel only, the opponent channels merely contributing to the "mental paint."

This analysis applies equally well to the trichromatic case.

APPENDIX D: EQUILUMINANT CONFIGURATIONS

Notice that for the equiluminant case, i.e., when $K==S$ (Appendix C), there is a very simple condition. That is to say, if the configuration is *known* to be equiluminant (which would be signaled by the absence of contrast in the achromatic channel), Metelli transparency can be decided on the basis of the opponent channel (which is the only channel carrying significant structural information in that case). This condition is that the opponent channels should have equal sign and that the contrast in the overlay should be lower than that in the background, thus

$$(LT > 0) \wedge (|T| < |L|). \tag{D1}$$

This strategy for deciding transparency is among the simplest, but applies only in roughly equiluminant displays. Note that these include strongly colored patterns.

ACKNOWLEDGMENTS

This work was sponsored in part via the European program Visiontrain contract MRTNCT2004005439 to JJK, with support also provided to WR by U.S. Air Force Office of Scientific Research (AFOSR) contract 6894705. Special thanks to S. M. Luria for his participation in the experiments; his observations and comments helped solidify our conclusions. We also thank the reviewers for a detailed examination of the text and appendices and for their suggestions that were most useful in clarifying the presentation.

REFERENCES

1. G. Wysecki and W. S. Stiles, *Color Science* (Wiley, 1967).
2. J. J. Koenderink, *Color for the Sciences* (MIT Press, 2009).
3. W. Richards and A. Witkin, "Transparency. Part II in efficient computations and representations of visible surfaces," W. Richards and K. Stevens, Final Report AFOSR Contract 79–0020, pp. 46–72, MIT Artificial Intelligence Laboratory (1979).
4. F. Metelli, "An algebraic development of the theory of transparency," Ergonomics **13**, 59–66 (1970).
5. F. Metelli, "The perception of transparency," Sci. Am. **230**, 90–98 (1974).
6. F. Metelli, "Achromatic color conditions in the perception of transparency," in *Perceptions: Essays in Honor of J J. Gibson*, R. B. MacLeod and H. L. Pick, eds. (Cornell University Press, 1974), pp. 96–116.
7. M. Brill, "Physical and informational constraints on the perception of transparency and translucency," Comput. Vis. Graph. Image Process. **28**, 356–362 (1984).
8. F. Metelli, S. C. Masin, and M. Manganelli, "Partial transparency," Atti dell' accademie Patavina di Scienze Lettere ed Arti **92**, 115–169 (1981).
9. J. Beck and R. Ivry, "On the role of figural organization in perceptual transparency," Percept. Psychophys. **44**, 585–594 (1988).
10. F. Metelli, O. da Pos, and A. Cavedon, "Balanced and unbalanced, complete and partial transparency," Percept. Psychophys. **38**, 354–366 (1985).
11. O. da Pos, *Trasparenze* (Icone, 1989).
12. T. Kozaki, M. Fukuda, Y. Nakano, and N. Masuda, "Phenomenal transparency and other related phenomena," Hiyoshi Rev. of Natural Science (Keio University) **6**, 68–81 (1989).
13. M. Fukuda and S. C. Masin, "Test of balanced transparency," Perception **23**, 37–43 (1994).
14. S. Masin, "The luminance conditions for transparency," Perception **26**, 39–50 (1997).
15. J. Beck, "Additive and subtractive mixture in color transparency," Percept. Psychophys. **23**, 256–267 (1978).
16. W. Gerbino, C. I. Stultiens, J. M. Troost, and C. M. de Weert, "Transparent layer constancy," J. Exp. Psychol. Hum. Percept. Perform. **16**, 3–20 (1990).
17. F. Faul and V. Ekroll, "Psychophysical model of chromatic perceptual transparency based on subtractive color mixture," J. Opt. Soc. Am. A **19**, 1084–1095 (2002).

18. S. Nakauchi, P. Silfsten, J. Parkkinen, and S. Ussui, "Computational theory of color transparency: recovery of spectral properties for overlapping surfaces," J. Opt. Soc. Am. A **16**, 2612–2624 (1999).
19. J. Hagedorn and M. D'Zmura, "Color appearance of surfaces viewed through fog," Perception **29**, 1169–1184 (2000).
20. B. G. Khang and Q. Zaidi, "Accuracy of color scission for spectral transparencies," J. Vision **2**, 451–466 (2002).
21. P. Kubelka and F. Munk, "Ein Beitrag zur Optik des Farbenstriche," Z. Tech. Phys. (Leipzig) **12**, 593 (1934).
22. P. Kubelka, "New contributions to the optics of intensely light-scattering materials. Part II. Nonhomogeneous layers," J. Opt. Soc. Am. **44**, 330–334 (1954).
23. J. Koenderink, A. van Doorn, S. Pont, and W. Richards, "Gestalt and phenomenal transparency," J. Opt. Soc. Am. A **25**, 190–202 (2008).
24. M. D'Zmura, P. Colantoni, K. Knoblauch, and B. Laget, "Color transparency," Perception **26**, 471–492 (1997).
25. W. Metzger, "Ueber Durchsichtigkeits-Erscheinungen," Rivista di Psicologia. Fascicolo Giubilare **49**, 187–189 (1955).
26. K. Nakayama, S. Shimojo, and V. S. Ramachandran, "Transparency: relations to depth, subjective contours, luminance and neon color spreading," Perception **19**, 497–513 (1990).
27. K. Nakayama and S. Shimojo, "Experiencing and perceiving visual surfaces," Science **257**, 1357–1363, (1992).
28. M. Singh and D. D. Hoffman, "Part boundaries alter the perception of transparency," Psychol. Sci. **9**, 370–378 (1988).
29. M. Singh and B. L. Anderson, "Toward a perceptual theory of transparency," Psychol. Rev. **109**, 492–519 (2002).
30. W. Richards, "Anomalous stereoscopic depth perception," J. Opt. Soc. Am. **61**, 410–414 (1971).
31. R. Van Ee and W. Richards, "A planar and volumetric test for stereoanomaly," Perception **31**, 51–64 (2002).
32. B. L. Anderson, "A theory of illusory lightness and transparency in monocular and binocular images," Perception **26**, 419–453 (1997).
33. V. J. Chen and M. D'Zmura, "Test of a convergence model for color transparency perception," Perception **27**, 595–608 (1988).
34. M. Singh and B. Anderson, "Photometric determinants of perceived transparency," Vision Res. **46**, 897–894 (2006).
35. B. L. Anderson, "The role of occlusion in the perception of depth, lightness and opacity," Psychol. Rev. **110**, 762–784 (2003).
36. M. Singh and B. L. Anderson, "Perceptual assignment of opacity to translucent surfaces: the role of image blur," Perception **31**, 531–552 (2002).
37. J. Wolfe, R. Birnkrant, M. Kunar, and T. Horowitz, "Visual search for transparencies and opacity: attentional guidance by cue combination?" J. Vision **5**, 257–274 (2005).
38. J. M. Fulvio, M. Singh, and L. T. Maloney, "Combining achromatic and chromatic cues to transparency," J. Vision **6**, 760–776 (2006).